

# Schrödinger Bridge for Generative Speech Enhancement

Ante Jukić, Roman Korostik, Jagadeesh Balam, Boris Ginsburg

NVIDIA, USA

{ajukic, rkorostik, jbalam, bginsburg}@nvidia.com

## Abstract

This paper proposes a generative speech enhancement model based on Schrödinger bridge (SB). The proposed model is employing a tractable SB to formulate a data-to-data process between the clean speech distribution and the observed noisy speech distribution. The model is trained with a data prediction loss, aiming to recover the complex-valued clean speech coefficients, and an auxiliary time-domain loss is used to improve training of the model. The effectiveness of the proposed SB-based model is evaluated in two different speech enhancement tasks: speech denoising and speech dereverberation. The experimental results demonstrate that the proposed SB-based outperforms diffusion-based models in terms of speech quality metrics and ASR performance, e.g., resulting in relative word error rate reduction of 20% for denoising and 6% for dereverberation compared to the best baseline model. The proposed model also demonstrates improved efficiency, achieving better quality than the baselines for the same number of sampling steps and with a reduced computational cost.

**Index Terms:** generative speech enhancement, speech denoising, speech dereverberation, Schrödinger bridge

## 1. Introduction

Recordings of speech signals are frequently corrupted by environmental noise, undesired sounds and room reverberation. The undesired signal components may impair the quality or intelligibility for human or machine listeners [1, 2]. The goal of speech enhancement (SE) in such scenarios is to recover the clean speech signal from a corrupted recording.

Typically, SE methods exploit statistical properties of the desired speech signal and the undesired disturbance signal. Classical model-based SE methods rely on a priori knowledge of the statistical properties of either one or both signals [3, 4]. Data-driven SE methods typically use machine learning (ML) models to learn signal properties from training data [5]. ML-based SE can be broadly divided into predictive and generative models. Predictive models aim to provide an estimate of the clean signal from the noisy signal, e.g., using an ML model to estimate real- or complex-valued spectral masks [6, 7], coefficients [8, 9] or the time domain signal [10]. Generative models aim to model the distribution of the clean signal given the noisy signal, e.g., using variational autoencoders [11, 12] or generative adversarial networks [13].

Recently, several diffusion-based generative models for SE have been proposed [14–23]. In general, diffusion-based models are based on two processes between the clean speech distribution and the noisy signal prior distribution [24]. The forward process transforms the clean data into a known prior distribution, and the reverse process starts from the prior distribution and generates an estimate of the clean speech. A neural network model is trained to guide the reverse process. In [14], spectrogram of the noisy signal was used as a conditioner for the

neural model, but only additive Gaussian noise was considered. A conditional diffusion model was proposed in [15] to handle non-Gaussian noise, with the diffusion process conditioned on the noisy signal. An alternative diffusion process in the short-time Fourier transform (STFT) domain was proposed in [17], enabling generative training of the model without any assumptions on the noise distribution. The proposed model operates on complex-valued time-frequency (TF) coefficients, enabling the neural model to learn the TF structure of the signal, and it has shown to be effective for speech denoising and dereverberation [19]. However, the model may produce hallucinations in adverse scenarios, resulting in vocalization or breathing artifacts in extreme noise or during speech absence [17, 18]. Prior mismatch of the diffusion process was reduced using modified objectives in [20, 22] and a modified forward process was used in [23]. A hybrid model, combining a predictive model and a diffusion-based generative model, was proposed in [18] to improve the robustness and reduce the computational complexity of the sampling process.

This paper proposes a generative SE model based on Schrödinger bridge (SB) [25–29]. As opposed to diffusion models, which describe data-to-noise process, the SB describes a data-to-data process. We consider a special case of SB where the clean speech and the noisy signal are considered as paired data [29]. The contribution of this work is threefold. Firstly, we propose a SE model based on Schrödinger bridge, using a SB for paired data [29]. As opposed to the noisy prior in diffusion-based models, the SB model results in a reverse process starting exactly from the observed noisy data. Secondly, we propose to combine the data prediction loss with an auxiliary loss to improve the performance of the proposed SB model. Thirdly, we demonstrate the effectiveness of the proposed approach in two different SE tasks: speech denoising and speech dereverberation. The results in terms of speech quality metrics and ASR performance demonstrate the effectiveness of the proposed approach, outperforming diffusion-based SE models at a lower computational complexity.

## 2. Background

Assuming a single static speech source, the signal captured by a single microphone can be modeled as  $\underline{y} = \underline{h} * \underline{x} + \underline{n}$ , where  $\underline{h}$  is the time-domain impulse response,  $\underline{x}$  is the clean speech signal, and  $\underline{n}$  is the additive noise signal. The goal of SE is to estimate the clean speech signal  $\underline{x} \in \mathbb{R}^N$  from the microphone signal  $\underline{y} \in \mathbb{R}^N$ . In the following,  $\mathbf{x} = \mathcal{A}(\underline{x}) \in \mathbb{C}^D$  denotes a vector of complex-valued coefficients obtained from the time-domain signal  $\underline{x}$ . The analysis transform  $\mathcal{A}$  is a composition of the STFT transform  $\mathcal{F}$  followed by scaling and compression, i.e.,  $\mathcal{A}(\mathbf{x}) = b|\mathcal{F}(\underline{x})|^a e^{j\angle \mathcal{F}(\underline{x})}$ , with element-wise operations, magnitude  $|\cdot|$  and angle  $\angle(\cdot)$ , compression coefficient  $a \in (0, 1]$ , and scale coefficient  $b > 0$  [17].

### 2.1. Score-based diffusion for speech enhancement

Score-based diffusion models [30, 31] are based on a continuous-time diffusion process defined by a forward stochastic differential equation (SDE)

$$d\mathbf{x}_t = \mathbf{f}(\mathbf{x}_t, t) dt + g(t) d\mathbf{w}_t, \quad \mathbf{x}_0 = \mathbf{x}, \quad (1)$$

where  $t \in [0, T]$  is the current time for the process,  $\mathbf{x}_t \in \mathbb{C}^D$  is the state of the process,  $\mathbf{f}$  is a vector-valued drift,  $g$  is a scalar-valued diffusion coefficient, and  $\mathbf{w}_t$  is the standard Wiener process. The corresponding reverse SDE can be expressed as [31]

$$d\mathbf{x}_t = [\mathbf{f}(\mathbf{x}_t, t) - g^2(t)\nabla \log p_t(\mathbf{x}_t)] dt + g(t) d\bar{\mathbf{w}}_t, \quad (2)$$

where  $\nabla \log p_t(\mathbf{x}_t)$  is the score function of the marginal distribution  $p_t$  at time  $t$ , and  $\bar{\mathbf{w}}_t$  is the reverse-time Wiener process. In [16, 17], the conditional relationship between the clean speech  $\mathbf{x}$  and the observed noisy speech  $\mathbf{y}$  was directly integrated in the SDE in (1) by using an affine drift term  $\mathbf{f}(\mathbf{x}_t, t) = \gamma(\mathbf{y} - \mathbf{x}_t)$  with stiffness parameter  $\gamma$ . Furthermore, a variance-exploding (VE) diffusion coefficient  $g(t) = \sqrt{ck^t}$  was used with scale  $c > 0$  and base  $k > 0$ , resulting in an Ornstein-Uhlenbeck SDE with VE (OUVE) [17]. The conditional transition distribution  $p_{t|0}$  for the state  $\mathbf{x}_t$  conditioned on the clean speech  $\mathbf{x}$  and the noisy observation  $\mathbf{y}$  can be expressed as

$$p_{t|0} = \mathcal{N}_{\mathbb{C}}(\boldsymbol{\mu}_x(t), \sigma_x^2(t)\mathbf{I}), \quad (3)$$

where  $\mathcal{N}_{\mathbb{C}}$  is a circularly-symmetric complex Gaussian distribution, and  $\mathbf{I}$  is the identity matrix. The mean  $\boldsymbol{\mu}_x(t)$  and the variance  $\sigma_x^2(t)$  in (3) are defined as

$$\boldsymbol{\mu}_x(t) = w_x(t)\mathbf{x} + w_y(t)\mathbf{y}, \quad \sigma_x^2(t) = \frac{c(k^{2t} - e^{-2\gamma t})}{2(\gamma + \log k)}, \quad (4)$$

with  $w_x(t) = e^{-\gamma t}$ ,  $w_y(t) = 1 - e^{-\gamma t}$  [17]. To enable inference using the reverse SDE in (2), the score function  $\nabla \log p_t(\mathbf{x}_t)$  is estimated using a neural network  $s_{\theta}$  with parameters  $\theta$  [17, 31]. The score function of the conditional transition distribution  $p_{t|0}$  can be computed analytically [30, 31], resulting in a denoising score matching training objective [17]

$$\min_{\theta} \mathcal{E}_{(\mathbf{x}, \mathbf{y}), t, \mathbf{z}} \|\sigma_x(t)s_{\theta}(\mathbf{x}_t, \mathbf{y}, t) - \mathbf{z}\|_2^2, \quad (5)$$

where  $\mathcal{E}$  is the mathematical expectation,  $\mathbf{x}_t = \boldsymbol{\mu}_x(t) + \sigma_x(t)\mathbf{z}$  and  $\mathbf{z} \sim \mathcal{N}_{\mathbb{C}}(0, \mathbf{I})$ , with the mean and variance in (4). The parameters  $\theta$  of the neural network are optimized by minimizing (5), with the expectation approximated by sampling  $(\mathbf{x}, \mathbf{y})$  from the training dataset,  $t$  uniformly from  $[t_{\min}, T]$  with a small  $t_{\min}$  to avoid numerical issues, and  $\mathbf{z}$  from a standard Gaussian distribution [17, 30, 31]. Inference is performed using the reverse SDE in (2) by using the estimated score  $s_{\theta}(\mathbf{x}_t, \mathbf{y}, t)$  and starting from an initial sample  $\mathbf{x}_T \sim \mathcal{N}_{\mathbb{C}}(\mathbf{y}, \sigma_x^2(T)\mathbf{I})$ .

## 3. Proposed model

### 3.1. Schrödinger bridge

We consider a Schrödinger bridge [25–29] defined as minimization of the Kullback-Leibler divergence  $D_{\text{KL}}$  between a path measure  $p$  and a reference path measure  $p_{\text{ref}}$ , subject to the boundary conditions

$$\min_{p \in \mathcal{P}_{[0, T]}} D_{\text{KL}}(p, p_{\text{ref}}) \quad \text{s. t.} \quad p_0 = p_x, \quad p_T = p_y, \quad (6)$$

where  $\mathcal{P}_{[0, T]}$  is the space of path measures on  $[0, T]$ . Assuming  $p_{\text{ref}}$  is defined by the reference forward SDE in (1), the SB is equivalent to a pair of forward-backwards SDEs [27, 29]

$$d\mathbf{x}_t = [\mathbf{f} + g^2(t)\nabla \log \Psi_t] dt + g(t) d\mathbf{w}_t, \quad \mathbf{x}_0 \sim p_x, \quad (7)$$

$$d\mathbf{x}_t = [\mathbf{f} - g^2(t)\nabla \log \bar{\Psi}_t] dt + g(t) d\bar{\mathbf{w}}_t, \quad \mathbf{x}_T \sim p_y, \quad (8)$$

Table 1: Noise schedules used for the proposed SB-based SE.

Noise schedule	Scaled VP	VE
$f(t)$	$-\frac{\beta_0 + (\beta_1 - \beta_0)t}{2}$	0
$g^2(t)$	$c[\beta_0 + (\beta_1 - \beta_0)t]$	$ck^{2t}$
$\alpha_t$	$e^{-\frac{1}{2}(\beta_0 t + \frac{\beta_1 - \beta_0}{2}t^2)}$	1
$\sigma_t^2$	$c\left(e^{\beta_0 t + \frac{\beta_1 - \beta_0}{2}t^2} - 1\right)$	$\frac{c(k^{2t} - 1)}{2 \log(k)}$

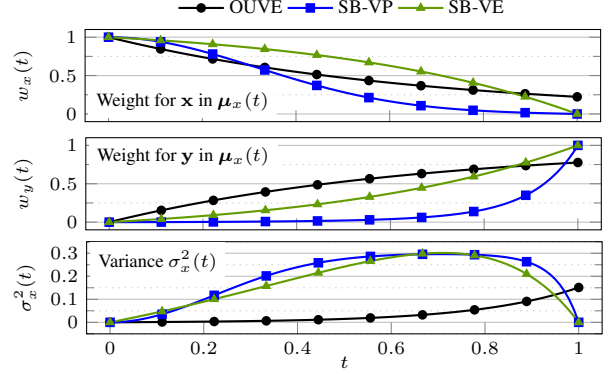


Figure 1: State  $\mathbf{x}_t$  mean  $\boldsymbol{\mu}_x(t)$  and variance  $\sigma_x^2(t)$  for OUVE noise schedule in (4) and SB noise schedules in (11),  $t \in [0, 1]$ .

where scores of  $\Psi, \bar{\Psi}_t$  are the optimal forward and reverse drifts, and some function arguments are omitted for brevity. The marginal distribution of the SB state  $\mathbf{x}_t$  can be expressed as  $p_t = \bar{\Psi}_t \Psi_t$  [27, 29]. While solving the SB is in general intractable, closed-form solutions exist for special cases, e.g., for Gaussian boundary conditions [28, 29].

### 3.2. Schrödinger bridge between paired data

Assume a linear drift  $\mathbf{f}(\mathbf{x}_t) = f(t)\mathbf{x}_t$  and Gaussian boundary conditions  $p_0 = \mathcal{N}_{\mathbb{C}}(\mathbf{x}, \epsilon_0^2\mathbf{I})$  and  $p_T = \mathcal{N}_{\mathbb{C}}(\mathbf{y}, \epsilon_T^2\mathbf{I})$  with  $\epsilon_T = e^{\int_0^T f(\tau) d\tau} \epsilon_0$ . When  $\epsilon_0 \rightarrow 0$ , the SB solution between clean data  $\mathbf{x}$  and noisy data  $\mathbf{y}$  can be expressed as [29]

$$\bar{\Psi}_t = \mathcal{N}_{\mathbb{C}}(\alpha_t \mathbf{x}, \alpha_t^2 \sigma_t^2 \mathbf{I}), \quad \Psi_t = \mathcal{N}_{\mathbb{C}}(\bar{\alpha}_t \mathbf{y}, \bar{\alpha}_t^2 \bar{\sigma}_t^2 \mathbf{I}), \quad (9)$$

with parameters  $\alpha_t = e^{\int_0^t f(\tau) d\tau}$ ,  $\sigma_t^2 = \int_0^t \frac{g^2(\tau)}{\alpha_\tau^2} d\tau$ ,  $\bar{\alpha}_t = \alpha_t \alpha_T^{-1}$  and  $\bar{\sigma}_t^2 = \sigma_T^2 - \sigma_t^2$ . Therefore, the marginal distribution  $p_t = \bar{\Psi}_t \Psi_t$  is also a Gaussian distribution which can be expressed as

$$p_t = \mathcal{N}_{\mathbb{C}}(\boldsymbol{\mu}_x(t), \sigma_x^2(t)\mathbf{I}). \quad (10)$$

The mean  $\boldsymbol{\mu}_x(t)$  and the variance  $\sigma_x^2(t)$  in (10) are defined as

$$\boldsymbol{\mu}_x(t) = w_x(t)\mathbf{x} + w_y(t)\mathbf{y}, \quad \sigma_x^2(t) = \frac{\alpha_t^2 \bar{\sigma}_t^2 \sigma_t^2}{\sigma_T^2}, \quad (11)$$

with  $w_x(t) = \alpha_t \bar{\sigma}_t^2 / \sigma_T^2$ , and  $w_y(t) = \bar{\alpha}_t \sigma_t^2 / \sigma_T^2$  [29].

Several different noise schedules defined by  $f(t)$  and  $g(t)$  have been considered in [29]. We use a variance preserving (VP) schedule with an additional scaling parameter  $c$  for the diffusion coefficient to match the variance of the diffusion-based models. Similarly as in Section 2.1, we also consider a VE diffusion coefficient with the drift term set to zero. Table 1 includes parametrization of the VP and VE noise schedules used here and expressions for their parameters  $\alpha_t$  and  $\sigma_t^2$ . Figure 1 shows the noise schedules used in Section 4 in terms of mean and variance evolution over time. As noted in [23], the OUVE schedule exhibits the mismatch of the mean at the final time

Table 2: Samplers for SB-based SE: solution  $\mathbf{x}_t$  at time  $t \in [0, \tau]$  given an initial value  $\mathbf{x}_\tau$  and  $\mathbf{z} \sim \mathcal{N}_{\mathbb{C}}(\mathbf{0}, \mathbf{I})$ .

SDE sampler (SB-SDE)	ODE sampler (SB-ODE)
$\mathbf{x}_t = \frac{\alpha_t \sigma_t^2}{\alpha_\tau \sigma_\tau^2} \mathbf{x}_\tau + \alpha_t \left(1 - \frac{\sigma_t^2}{\sigma_\tau^2}\right) \hat{\mathbf{x}}_\theta(\tau) + \alpha_t \sigma_t \sqrt{1 - \frac{\sigma_t^2}{\sigma_\tau^2}} \mathbf{z}$	$\mathbf{x}_t = \frac{\alpha_t \sigma_t \bar{\sigma}_t}{\alpha_\tau \sigma_\tau \bar{\sigma}_\tau} \mathbf{x}_\tau + \frac{\alpha_t}{\sigma_\tau^2} \left(\bar{\sigma}_t^2 - \frac{\bar{\sigma}_\tau \sigma_t \bar{\sigma}_t}{\sigma_\tau}\right) \hat{\mathbf{x}}_\theta(\tau) + \frac{\alpha_t}{\alpha_\tau \sigma_\tau^2} \left(\sigma_t^2 - \frac{\sigma_\tau \sigma_t \bar{\sigma}_t}{\sigma_\tau}\right) \mathbf{y}$

$t = 1$ . Due to the constraints in (6), the mean for both SB schedules exactly interpolates between the clean data  $\mathbf{x}$  at  $t = 0$  and the noisy data  $\mathbf{y}$  at  $t = 1$ . Note that the VE and VP schedules have a similar variance evolution, but different mean evolution.

### 3.3. Model training

As noted in [29], the backbone neural model can be trained to match the score  $\nabla \log p_t$ , to predict the noise using  $\nabla \log \bar{\Psi}_t$ , or to predict the data  $\mathbf{x}$ . We consider the data prediction loss, since it performed well in [29]. Additionally, we propose to use an auxiliary loss  $\mathcal{L}_{\text{aux}}$  to improve the estimate of the model, resulting in the following training objective

$$\min_{\theta} \mathcal{E}_{(\mathbf{x}, \mathbf{y}), t, \mathbf{z}} \frac{1}{D} \|\hat{\mathbf{x}}_\theta(t) - \mathbf{x}\|_2^2 + \lambda \mathcal{L}_{\text{aux}}(\hat{\mathbf{x}}_\theta(t), \mathbf{x}), \quad (12)$$

where  $\hat{\mathbf{x}}_\theta(t) = d_\theta(\mathbf{x}_t, \mathbf{y}, t)$  is the current estimate using a neural network  $d_\theta$ ,  $\hat{\mathbf{x}}_\theta(t) = \mathcal{A}^{-1}(\hat{\mathbf{x}}_\theta(t))$  is the corresponding time-domain signal, and  $\lambda > 0$  is a tradeoff parameter. Using  $\lambda = 0$  recovers the original data prediction loss. In Section 4.3, we report results using the  $\ell_1$ -norm  $\mathcal{L}_{\text{aux}}(\hat{\mathbf{x}}, \mathbf{x}) = \frac{1}{N} \|\hat{\mathbf{x}} - \mathbf{x}\|_1$ . Note that we obtained a similar performance using the negative soft-thresholded SI-SDR [32].

### 3.4. Inference

The reverse SDE in (8) can be expressed in terms of the current state  $\mathbf{x}_t$  and the current neural estimate  $\hat{\mathbf{x}}_\theta(t)$  by computing  $\nabla \log \bar{\Psi}_t$  from (9) and replacing  $\mathbf{x}$  with  $\hat{\mathbf{x}}_\theta(t)$  [29]. Given an initial value  $\mathbf{x}_\tau$  at time  $\tau > 0$ , the solution of the resulting bridge SDE (8) at time  $t \in [0, \tau]$  can be obtained using first-order discretization in Table 2. Similarly, a probability flow ordinary differential equation (ODE) formulation can be used to solve the bridge ODE [29], resulting in an ODE sampler in Table 2. For both the samplers in Table 2, the reverse process starts from  $\mathbf{x}_T = \mathbf{y}$ , and the final estimate  $\hat{\mathbf{x}} = \mathbf{x}_0$  is obtained after a number of steps. The time-domain output signal is obtained by inverting the analysis transform as  $\hat{\mathbf{x}} = \mathcal{A}^{-1}(\hat{\mathbf{x}})$ .

## 4. Experiments

### 4.1. Datasets

We consider two enhancement tasks: speech denoising and speech dereverberation. For the speech denoising task, we prepared the WSJ0-CHiME3 dataset similarly as in [18]. The dataset was generated using WSJ clean speech [33] and CHiME3 noise [34] and the mixture SNR was sampled uniformly in  $[-6, 14]$  dB [18]. Approximately 13k utterances (25 h) were generated for the training set, 1.2k utterances (2 h) for the validation set and 650 utterances (1.5 h) for the test set. For the speech dereverberation task, we prepared the WSJ0-Reverb dataset similarly as in [18]. The dataset was generated by convolving WSJ clean speech [33] with room impulse responses (RIRs) simulated using the image method [35]. Room width and length were sampled uniformly in  $[5, 15]$  m, and height was sampled in  $[2, 6]$  m. Source and microphone locations were selected randomly in the room with a minimum distance of 1 m from the closest wall. Reverberation time was sampled in  $[0.4, 1.0]$  s, and the corresponding anechoic RIR for generating the target signal was generated using a fixed absorption coefficient 0.99. The sampling rate was 16 kHz.

Table 3: Speech denoising performance on WSJ0-CHiME3. Values are reported as mean  $\pm$  standard deviation.

Signal	PESQ $\uparrow$	ESTOI $\uparrow$	SI-SDR/dB $\uparrow$	WER/% $\downarrow$
Clean	—	—	—	3.03
Unprocessed	$1.35 \pm 0.30$	$0.63 \pm 0.18$	$4.0 \pm 5.8$	12.18
NCSN++	$2.18 \pm 0.65$	<b><math>0.88 \pm 0.09</math></b>	<b><math>16.1 \pm 4.5</math></b>	5.39
SGMSE+	$2.28 \pm 0.60$	$0.85 \pm 0.11$	$13.1 \pm 4.9$	9.52
StoRM	$2.53 \pm 0.60$	$0.87 \pm 0.09$	$14.8 \pm 4.3$	5.39
SB-VP	<b><math>2.62 \pm 0.56</math></b>	<b><math>0.88 \pm 0.07</math></b>	$14.9 \pm 4.3$	<b>4.69</b>
SB-VE	$2.58 \pm 0.53$	<b><math>0.88 \pm 0.07</math></b>	$14.7 \pm 4.2$	5.10

Table 4: Speech dereverberation performance on WSJ0-Reverb. Values are reported as mean  $\pm$  standard deviation.

Signal	PESQ $\uparrow$	ESTOI $\uparrow$	SI-SDR/dB $\uparrow$	WER/% $\downarrow$
Clean	—	—	—	3.64
Unprocessed	$1.29 \pm 0.13$	$0.44 \pm 0.11$	$-9.5 \pm 6.3$	8.29
NCSN++	$2.00 \pm 0.45$	$0.83 \pm 0.06$	$5.2 \pm 4.2$	6.45
SGMSE+	$2.34 \pm 0.43$	$0.82 \pm 0.07$	$0.0 \pm 8.9$	5.84
StoRM	$2.52 \pm 0.41$	$0.85 \pm 0.05$	$5.6 \pm 4.3$	<b>4.69</b>
SB-VP	$2.26 \pm 0.46$	$0.80 \pm 0.08$	$4.1 \pm 3.9$	8.62
SB-VE	<b><math>2.68 \pm 0.41</math></b>	<b><math>0.87 \pm 0.05</math></b>	<b><math>6.6 \pm 3.7</math></b>	5.91

### 4.2. Experimental setup

The analysis transform  $\mathcal{A}$  is computed using the STFT window size of 510 samples, hop size of 128 samples, and compression parameters  $a = 0.5$  and  $b = 0.33$  [18]. The proposed Schrödinger bridge model is denoted as SB, and it is trained using the data prediction loss in (12) with  $\lambda = 0$ , unless stated otherwise, and either VP or VE noise schedule as in Figure 1. The VE schedule used  $k = 2.6$ ,  $c = 0.40$ , achieving the maximum variance  $\sigma_x^2(t)$  of 0.3, twice as large as the maximum OUVE variance of 0.15, similarly as in [23]. The VP schedule used  $\beta_0 = 0.01$ ,  $\beta_1 = 20$  as in [29] with variance scale  $c = 0.3$ , achieving the same maximum variance as VE. Process time for the proposed SB is set to  $T = 1$  with  $t_{\min} = 10^{-4}$ . Backbone neural network for the SB models is the noise-conditional score network (NCSN++) proposed in [31] with approximately 25.2 M parameters. The model is using four down-sampling and up-sampling steps with the configuration following [18]. Training is performed on randomly-selected audio segments corresponding to 256 STFT frames, and the input and the target signals are normalized with the maximum amplitude of the input signal. The global batch size was set to 64 and the optimizer was Adam with learning rate  $10^{-4}$  [18]. All models are trained on eight NVIDIA V100 GPUs for a maximum of 1000 epochs with early stopping based on the validation SI-SDR evaluated every 5 epochs and patience of 20 epochs. We use exponential moving average (EMA) of the weights with decay 0.999 [18], and the best EMA checkpoint is selected based on the PESQ value of 50 validation examples [17, 18]. Inference is using 50 time steps, unless stated otherwise, with a uniform grid across time. All models are implemented in NVIDIA’s NeMo toolkit [36].

The proposed model is compared to three baseline models. Firstly, we consider a predictive model denoted as NSCN++ [17, 18], trained to directly estimate the clean speech coefficients  $\hat{\mathbf{x}}$  from  $\mathbf{y}$  [17, 18]. Secondly, we consider a diffusion-based generative model denoted as SGMSE+, trained using score matching (5) with NCSN++ as the backbone [17,

Table 5: Performance of SB-VE on WSJ0-CHiME3 and WSJ0-Reverb trained with  $\mathcal{L}_{aux}$  and using different samplers for inference.

$\mathcal{L}_{aux}$	Sampler	WSJ0-CHiME3				WSJ0-Reverb			
		PESQ $\uparrow$	ESTOI $\uparrow$	SI-SDR/dB $\uparrow$	WER/% $\downarrow$	PESQ $\uparrow$	ESTOI $\uparrow$	SI-SDR/dB $\uparrow$	WER/% $\downarrow$
$\lambda = 0$	SDE	2.58 $\pm$ 0.53	0.88 $\pm$ 0.07	14.7 $\pm$ 4.2	5.10	2.68 $\pm$ 0.41	0.87 $\pm$ 0.05	6.6 $\pm$ 3.7	5.91
	ODE	2.16 $\pm$ 0.60	<b>0.90 <math>\pm</math> 0.07</b>	<b>16.3 <math>\pm</math> 4.2</b>	5.13	2.19 $\pm$ 0.49	<b>0.89 <math>\pm</math> 0.04</b>	<b>8.4 <math>\pm</math> 3.5</b>	5.29
$\ell_1$ -norm, $\lambda = 10^{-3}$	SDE	2.64 $\pm$ 0.55	0.89 $\pm$ 0.07	14.8 $\pm$ 4.2	4.96	<b>2.77 <math>\pm</math> 0.41</b>	<b>0.89 <math>\pm</math> 0.04</b>	7.1 $\pm$ 3.9	<b>4.38</b>
	ODE	<b>2.81 <math>\pm</math> 0.52</b>	<b>0.90 <math>\pm</math> 0.07</b>	16.1 $\pm$ 4.1	<b>4.19</b>	2.58 $\pm$ 0.46	0.85 $\pm$ 0.06	5.4 $\pm$ 4.9	6.29

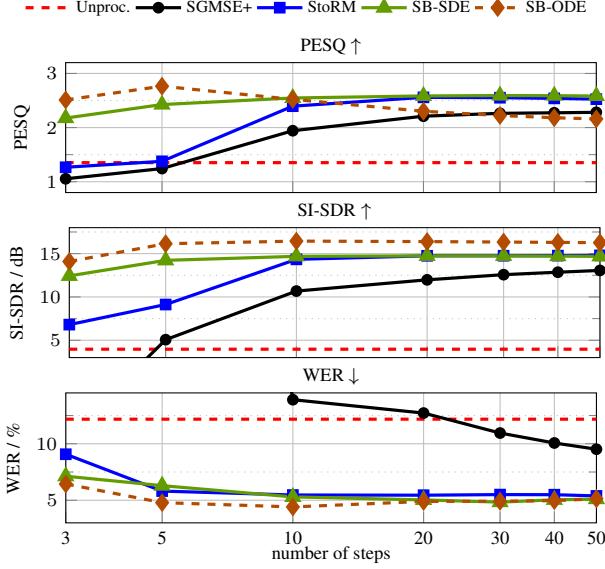


Figure 2: Speech denoising on WSJ0-CHiME3 with different numbers of sampling steps and either SB-SDE or SB-ODE in Table 2. Note that some results for SGMSE+ are out of range.

18]. Thirdly, we consider a hybrid stochastic regeneration model denoted as StoRM [18], consisting of a predictive NCSN++ module and a diffusion-based SGMSE+ module. The baseline models were implemented and trained in our framework. However, the results reported in Section 4.3 were obtained using pre-trained checkpoints from [18], since they were slightly better (approximately 0.05 in PESQ and 0.3 dB SI-SDR on WSJ0-CHiME3).

The performance is evaluated in terms of perceptual evaluation of speech quality (PESQ) [37], extended short-term objective intelligibility (ESTOI) [38], scale-invariant signal-to-distortion ratio (SI-SDR) [39] and word error rate (WER). Clean speech at the microphone was the reference for signal-based metrics. For WER evaluation we used NVIDIA’s FastConformer-Transducer-Large English ASR model [40]. Test examples are available online.<sup>1</sup>

### 4.3. Results

Table 3 shows the test performance of the models trained on WSJ0-CHiME3. Predictive NCSN++ achieved the best performance in terms of SI-SDR, as also noted in [17, 18]. The proposed SB outperformed the diffusion-based SGMSE+ model in terms of signal quality and ASR performance by a large margin. Furthermore, SB performed better or on par with the hybrid StoRM model, without using a separate predictive model. In general, SB resulted in significantly less hallucinations than SGMSE+ and performed similarly to StoRM. SB-VE and SB-VP performed similarly in terms of signal quality metrics, with the latter achieving a better ASR performance.

Table 4 shows the test performance of the models trained

on WSJ0-Reverb. The proposed SB-VE outperformed the diffusion-based SGMSE+ model in terms of signal quality, while achieving a similar ASR performance. The proposed SB-VE performed better than the hybrid StoRM model in signal quality metrics, although it lagged in ASR evaluation. In this task, SB-VP performed worse than SB-VE in all metrics. Since SB-VE performed well in both tasks, it was used for the rest of the experiments.

Table 5 shows the performance of the SB-VE model with different samplers and with the auxiliary loss. With data prediction loss ( $\lambda = 0$ ), the ODE sampler performed well in terms of ESTOI, SI-SDR and WER. However, the SDE sampler performed significantly better in terms of PESQ. The tradeoff parameter  $\lambda$  in (12) was selected from  $10^{\{-4, \dots, 1\}}$  and  $\lambda = 10^{-3}$  showed a good validation performance. With  $\mathcal{L}_{aux}$ , the results for both SDE and ODE sampler were mostly improved across the board. The best result on WSJ0-CHiME3 is achieved using the ODE sampler, outperforming the best baseline StoRM in Table 3 in all metrics, resulting in a relative WER reduction of more than 20%. The best result on WSJ0-Reverb is achieved using the SDE sampler, outperforming the best baseline StoRM in Table 3 in all metrics, resulting in a relative WER reduction of more than 6%.

Finally, the influence of the number of steps for the reverse process for WSJ0-CHiME3 is investigated in Figure 2. SB is using the same SB-VE model and only the sampler is changed at inference time. It can be observed that SB is more robust to the number of steps used in the reverse process, performing significantly better than the baseline diffusion SGMSE+ and the hybrid StoRM models. The performance gap is especially large for WER, where SGMSE+ performs poorly as the number of steps is reduced. Furthermore, SB performs better than the hybrid StoRM model, especially for a small number of steps, without a separate predictive model. Interestingly, SB-ODE shows an improved performance in PESQ and WER for a small number of steps, while still performing well in SI-SDR. Note that the baseline SGMSE+ and StoRM models are using the same number of steps, but they employ a predictor-corrector sampler, which performs two calls to backbone neural networks per step [17, 18]. The proposed SB models with samplers from Table 2 perform only one call to the backbone neural network per step, resulting in a significant reduction in computational complexity.

## 5. Conclusions

In this paper, we presented a speech enhancement model based on the Schrödinger bridge. As opposed to diffusion-based models, the proposed model is based on a data-to-data process. The proposed model outperforms both diffusion-only baseline and a hybrid baseline, combining predictive and generative models, both in terms of signal quality and ASR performance. In general, very good performance has been observed across the tested conditions, e.g., with relative WER reduction of more than 20% for denoising and 6% for dereverberation compared to the best baseline model. Furthermore, the proposed SB model is more robust to the number of steps used in the reverse process, performing significantly better than the baseline models.

<sup>1</sup><https://tauaxdefbe.github.io/demo>

## 6. References

- [1] R. Beutelmann and T. Brand, "Prediction of speech intelligibility in spatial noise and reverberation for normal-hearing and hearing-impaired listeners," *The Journal of the Acoustical Society of America*, vol. 120, no. 1, pp. 331–342, 2006.
- [2] T. Yoshioka *et al.*, "Making machines understand us in reverberant rooms: Robustness against reverberation for automatic speech recognition," *IEEE Signal Process. Magazine*, vol. 29, no. 6, pp. 114–126, 2012.
- [3] R. C. Hendriks, T. Gerkmann, and J. Jensen, *DFT-domain based single-microphone noise reduction for speech enhancement*. Springer, 2013.
- [4] T. Gerkmann and E. Vincent, "Spectral masking and filtering," in *Audio source separation and speech enhancement*, E. Vincent, T. Virtanen, and S. Gannot, Eds., 2018, pp. 65–85.
- [5] D. Wang and J. Chen, "Supervised speech separation based on deep learning: An overview," *IEEE/ACM Trans. on Audio, Speech, and Language Process.*, vol. 26, no. 10, pp. 1702–1726, 2018.
- [6] Y. Wang, A. Narayanan, and D. Wang, "On training targets for supervised speech separation," *IEEE/ACM Trans. on Audio, Speech, and Language Process.*, vol. 22, no. 12, pp. 1849–1858, 2014.
- [7] D. S. Williamson, Y. Wang, and D. Wang, "Complex ratio masking for monaural speech separation," *IEEE/ACM Trans. on Audio, Speech, and Language Process.*, vol. 24, no. 3, pp. 483–492, 2015.
- [8] Y. Xu *et al.*, "A regression approach to speech enhancement based on deep neural networks," *IEEE/ACM Trans. on Audio, Speech, and Language Process.*, vol. 23, no. 1, pp. 7–19, 2014.
- [9] K. Han *et al.*, "Learning spectral mapping for speech dereverberation and denoising," *IEEE/ACM Trans. on Audio, Speech, and Language Process.*, vol. 23, no. 6, pp. 982–992, 2015.
- [10] Y. Luo and N. Mesgarani, "Tasnet: time-domain audio separation network for real-time, single-channel speech separation," in *Proc. IEEE Int. Conf. on Acoustics, Speech and Signal Process. (ICASSP)*, 2018, pp. 696–700.
- [11] D. P. Kingma and M. Welling, "Auto-encoding variational Bayes," *arXiv preprint arXiv:1312.6114*, 2013.
- [12] S. Leglaive, L. Girin, and R. Horaud, "A variance modeling framework based on variational autoencoders for speech enhancement," in *Proc. Int. Workshop on Machine Learning for Signal Process. (MLSP)*. IEEE, 2018, pp. 1–6.
- [13] S. Pascual, A. Bonafonte, and J. Serra, "SEGAN: Speech enhancement generative adversarial network," in *Proc. Interspeech*, 2017.
- [14] Y.-J. Lu, Y. Tsao, and S. Watanabe, "A study on speech enhancement based on diffusion probabilistic model," in *Proc. Asia-Pacific Signal and Inform. Process. Assoc. Annual Summit and Conf. (APSIPA ASC)*, 2021, pp. 659–666.
- [15] Y.-J. Lu *et al.*, "Conditional diffusion probabilistic model for speech enhancement," in *Proc. IEEE Int. Conf. on Acoustics, Speech and Signal Process. (ICASSP)*, 2022, pp. 7402–7406.
- [16] S. Welker, J. Richter, and T. Gerkmann, "Speech enhancement with score-based generative models in the complex STFT domain," in *Proc. Interspeech*, 2022.
- [17] J. Richter *et al.*, "Speech Enhancement and Dereverberation with Diffusion-Based Generative Models," *IEEE/ACM Trans. on Audio, Speech, and Language Process.*, vol. 31, pp. 2351–2364, 2023.
- [18] J.-M. Le Mercier *et al.*, "StoRM: A Diffusion-based Stochastic Regeneration Model for Speech Enhancement and Dereverberation," *IEEE/ACM Trans. on Audio, Speech, and Language Process.*, vol. 31, pp. 2724–2737, 2023.
- [19] —, "Analysing Diffusion-based Generative Approaches Versus Discriminative Approaches for Speech Restoration," in *Proc. IEEE Int. Conf. on Acoustics, Speech and Signal Process. (ICASSP)*, Jun. 2023.
- [20] R. Scheibler *et al.*, "Diffusion-based generative speech source separation," in *Proc. IEEE Int. Conf. on Acoustics, Speech and Signal Process. (ICASSP)*, 2023.
- [21] Z. Guo *et al.*, "Variance-preserving-based interpolation diffusion models for speech enhancement," in *Proc. Interspeech*, 2023.
- [22] N. Kamo, M. Delcroix, and T. Nakatani, "Target Speech Extraction with Conditional Diffusion Model," in *Proc. Interspeech*, 2023, pp. 176–180.
- [23] B. Lay *et al.*, "Reducing the Prior Mismatch of Stochastic Differential Equations for Diffusion-based Speech Enhancement," in *Proc. Interspeech*, Aug. 2023.
- [24] L. Yang *et al.*, "Diffusion models: A comprehensive survey of methods and applications," *ACM Computing Surveys*, vol. 56, no. 4, pp. 1–39, 2023.
- [25] E. Schrödinger, "Sur la théorie relativiste de l'électron et l'interprétation de la mécanique quantique," in *Annales de l'institut Henri Poincaré*, vol. 2, no. 4, 1932, pp. 269–310.
- [26] V. De Bortoli *et al.*, "Diffusion Schrödinger bridge with applications to score-based generative modeling," in *Proc. NeurIPS*, 2021.
- [27] T. Chen, G.-H. Liu, and E. A. Theodorou, "Likelihood training of Schrödinger bridge using forward-backward SDEs theory," in *Proc. ICLR*, 2022.
- [28] C. Bunne *et al.*, "The Schrödinger bridge between Gaussians measures has a closed form," in *Proc. Int. Conf. on Artificial Intell. and Stat. (AISTATS)*, 2023.
- [29] Z. Chen, G. He, K. Zheng, X. Tan, and J. Zhu, "Schrödinger Bridges Beat Diffusion Models on Text-to-Speech Synthesis," *arXiv preprint arXiv:2312.03491*, Dec. 2023.
- [30] Y. Song and S. Ermon, "Generative modeling by estimating gradients of the data distribution," in *Proc. NeurIPS*, 2019.
- [31] Y. Song *et al.*, "Score-based generative modeling through stochastic differential equations," in *Proc. Int. Conf. Learning Representations (ICLR)*, May 2021.
- [32] S. Wisdom *et al.*, "Unsupervised sound separation using mixture invariant training," *Proc. Neural Information Proc. Systems (NeurIPS)*, vol. 33, pp. 3846–3857, 2020.
- [33] J. S. Garofolo *et al.*, "CSR-I (WSJ0) Complete," <https://catalog.ldc.upenn.edu/LDC93S6A>, [Online].
- [34] J. Barker *et al.*, "The third 'CHiME' speech separation and recognition challenge: Analysis and outcomes," *Computer Speech & Language*, vol. 46, pp. 605–626, 2017.
- [35] R. Scheibler, E. Bezzam, and I. Dokmanić, "Pyroomacoustics: A Python package for audio room simulations and array processing algorithms," in *Proc. IEEE Int. Conf. on Acoustics, Speech and Signal Process. (ICASSP)*, 2018.
- [36] NVIDIA, "NeMo: a toolkit for conversational AI," <https://github.com/NVIDIA/NeMo>, [Online].
- [37] A. Rix *et al.*, "Perceptual evaluation of speech quality (PESQ) - a new method for speech quality assessment of telephone networks and codecs," in *Proc. IEEE Int. Conf. on Acoustics, Speech and Signal Process. (ICASSP)*, 2001.
- [38] J. Jensen and C. H. Taal, "An Algorithm for Predicting the Intelligibility of Speech Masked by Modulated Noise Maskers," *IEEE/ACM Trans. on Audio, Speech, and Language Process.*, vol. 24, no. 11, pp. 2009–2022, Dec. 2016.
- [39] J. Le Roux *et al.*, "SDR - half-baked or well done?" in *Proc. IEEE Int. Conf. on Acoustics, Speech and Signal Process. (ICASSP)*, 2019.
- [40] NVIDIA, "STT En Fast Conformer-Transducer Large," [https://catalog.ngc.nvidia.com/orgs/nvidia/teams/nemo/models/stt\\_en\\_fastconformer-transducer-large](https://catalog.ngc.nvidia.com/orgs/nvidia/teams/nemo/models/stt_en_fastconformer-transducer-large), 2023, [Online; accessed Feb-2024].